Computational Materials Science 139 (2017) 1–7

Contents lists available at ScienceDirect

Computational Materials Science

journal homepage: www.elsevier.com/locate/commatsci

Ab initio study of *F*-centers in alkali halides

J. Hoya [a,b], J.I. Laborde [a], D. Richard [a,b,*], M. Rentería [a,b]

[a] Departamento de Física, Facultad de Ciencias Exactas, Universidad Nacional de La Plata, CC 67, 1900 La Plata, Argentina
[b] Instituto de Física La Plata (IFLP, CCT La Plata, CONICET-UNLP), Facultad de Ciencias Exactas, Universidad Nacional de La Plata, CC 67, 1900 La Plata, Argentina

ARTICLE INFO

Article history:
Received 1 June 2017
Received in revised form 6 July 2017
Accepted 16 July 2017

Keywords:
Alkali halide
F-center
DFT
Ab initio
Defect level

ABSTRACT

The structural and electronic properties of an electron trapped at vacant anion site in alkali halides are investigated using first principles electronic structure calculations with the supercell method. In order to determine the spatial electronic charge density and band structure of the studied systems we used the Augmented Plane Waves plus local orbital (APW + lo) method in the framework of the Density Functional Theory (DFT), considering the Wu and Cohen parametrization of the generalized gradient approximation (WCGGA) for the exchange and correlation energy, and the modification of Tran and Blaha to the Becke and Johnson exchange potential (mBJ method). We discuss the improvements in the description of the defect levels induced by the vacancies using mBJ compared to WCGGA. Additionally, we revisit the experiment to perform a new determination of the UV/Vis absorption energies in *F*-centers. In the theoretical framework used, we demonstrate that the bound electron at the *F*-center is localized within a sphere with diameter twice the lattice parameter. From the comparison of our theoretical predictions with the Mollwo-Ivey relation that comes from this new experiment, we show that the mBJ method predicts accurately the energy band gaps and gives better energy values for the *s*-*p* transitions that give rise to the optical absorption energies.

1. Introduction

The *F*-center is a lattice defect which consists of an electron bound at a vacant negative ion site. It is the simplest defect that can occur in ionic crystals like the alkali halides, when halogen vacancies are produced by, for example, X-ray irradiation [1,2]. In these cases, when an anion is removed from the host crystal, it is replaced by an electron that occupies a donor state of a_{1g}-like symmetry in the ground state (*s*-type state). The electronic transition to a defect-induced level of t_{1u} symmetry (*p*-type state) explains the optical absorption energy peaks observed for *F*-centers in UV–Vis absorption experiments. In this way, the fundamental optical absorption energies arise from electronic transitions from the lowest 1*s* to 2*p* bound levels, according to the dipole selection rule. Many experimental and theoretical efforts have been done from the very beginning to study *F*-centers [2,3]. More recently, many *ab initio* methods were used in order to predict structural and electronic properties of the anion vacancies in alkali halides [4–10]. However, the study of *F*-centers by first-principles goes beyond the rocksalt structure, and it has been applied to a wide variety of structures. Among them, we can find, for example, bulk calculations in fluorite [11–13], perovskite [14,15], rutile [16–18], and anastase [18] structures, which gave a description of the *F*-center with different degrees of success depending on the used *ab initio* approach.

In this work, the UV/VIS absorption experiment was revisited for a variety of alkali halides, and we present a systematic *ab initio* structural and electronic band structure study for the following compounds: KI, KBr, KCl, NaCl, LiCl, NaF, and LiF. To this purpose we used the WIEN2k implementation of the Augmented Plane Wave plus local orbitals (APW + lo) method, in the framework of the DFT [19]. For the exchange and correlation energy, we first considered the Wu and Cohen parametrization of the generalized gradient approximation (WCGGA) [20]. Because it is known that this approximation systematically subestimates the energy band gaps E_g for most semiconductors [21], we also used the modified version of the Becke and Johnson exchange potential proposed by Tran and Blaha (mBJ method), which gives very accurate values of E_g in most semiconductors and insulators [22–24]. For the alkali halides that are subject of this study, we analyze how the improvements in the prediction of the E_g energies using the mBJ method affect the position of the defect levels when halogen vacancies are produced, and how better the electronic band structure is correlated with the experimental optical response in *F*-centers. To our knowledge, this

* Corresponding author at: Instituto de Física La Plata (IFLP, CCT La Plata, CONICET-UNLP), Facultad de Ciencias Exactas, Universidad Nacional de La Plata, CC 67, 1900 La Plata, Argentina.
E-mail address: richard@fisica.unlp.edu.ar (D. Richard).

http://dx.doi.org/10.1016/j.commatsci.2017.07.015
0927-0256/

is the first time the APW + lo method is systematically applied to the study of these systems in this way.

2. Experimental procedure

The *F*-centers in the samples were prepared by the method of ionizing radiation, using X-rays. Alkali halide single crystals were irradiated for about 5 min at room temperature and normal pressure using the X-ray tube (at 40 kV, 30 mA, with a rhodium anode) of a Philips Wavelength X-ray (fluorescence) spectrometer at YPF Technological Center (Ensenada, Argentina). The absorption spectra were measured at room temperature in air using a UV–Vis Cintra 20 double-beam spectrophotometer (GBC Scientific Equipment Ltd.), ranging from 300 to 850 nm in 0.427 nm steps, except for LiF, where the 190–900 nm range was used. The slit-width was set to 0.8 nm and both deuterium and tungsten-iodine lamps were used to cover this wavelength range. A Ho_2O_3 glass sample was previously used as wavelength standard for calibration of the spectrophotometer. In Fig. 1 we present the obtained spectra. For each compound, the absorption energy E_a was obtained from the corresponding spectrum by a Gaussian fitting after subtracting a linear background. The results for E_a are presented in Table 1 (fourth column) and plotted in Fig. 2. These measured values are in very good agreement with those reported by other authors [2]. According to our results, we obtained the empirical Mollwo-Ivey relation:

$$E_a(d) = 16.5(9)d^{-1.76(6)} \quad (1)$$

where d is the interionic distance in Å and E_a is expressed in eV.

3. First-principles calculations

3.1. Perfect crystal

The studied alkali halides have the well-known cubic NaCl-like structure (rocksalt), which consists in a face-centered cubic (fcc) array of cations with an interpenetrating fcc anion array (see Fig.3a) [25].

In order to perform the APW + lo calculations, the muffin tin radii (R_{MT}) were chosen in order to allow the relaxation of the structure maintaining non-overlapping atomic spheres (for this purpose we choose R_{MT} values 5% lower than $d/2$). We used R_{MT}-K_{max} = 7 (parameter that controls the size of the basis of eigenfunctions) and 100 k points in the full Brillouin zone, having prior verification of the convergence in the total energy of each system. Once self-consistency of the potential was achieved, the forces on the ions were obtained, and they were moved according to a Newton damped scheme until the forces on the ions were below 0.005 eV/A. This procedure was performed with the WCGGA approximation, which allows the determination of the equilibrium atomic positions (*relaxed structure*), because it provides a functional for the exchange and correlation energy. The relaxed structures obtained by WCGGA were then considered for the calculations with the mBJ method, which does not allow calculating the equilibrium positions.

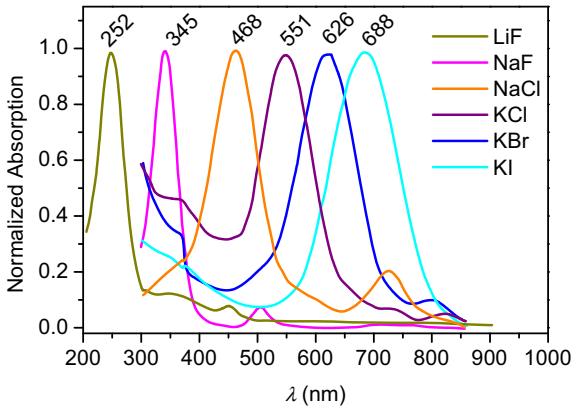

Fig. 1. Normalized absorption spectra for the studied compounds. The peak maxima are indicated in nm.

The density of electronic states (DOS) of NaCl using the WCGGA approximation is shown in Fig. 4a. This system was taken as a representative example of all the studied systems. Fig. 4b and c shows the atom-projected partial DOS for Na and Cl atoms, respectively. According to these figures, the valence band of NaCl is dominated by Cl-3*p* states, with a small contribution of Na orbitals, in agreement with the predominantly ionic nature of this alkali halide. As can be seen there, the conduction band bottom has both Na-*s* and Cl-*s* character, with an admixture of *p* states. The WCGGA calculations predict a band gap of 5.3 eV, which is smaller than the experimental one (8.5(2) eV [26]). Similar results were obtained in the other studied pure alkali halides with WCGGA, *i.e.* the cation and the anion in each alkali halide contribute to the DOS in a similar way to that presented for Na and Cl, respectively. The overall band structures obtained are consistent with previous theoretical results obtained in these systems [27–29]. The Fig. 4d–f shows the total and atom-projected partial DOS for pure NaCl using the mBJ method. This potential diminishes the valence-band width and increases the energy band-gap with respect to those calculated with WCGGA. However, it does not change substantially the internal band structure (see Fig. 4e and f). In this case, using mBJ the calculated band-gap is E_g^{pure} = 8.4 eV, which is in very good agreement with previous calculations [23]. In Table 1 we present the corresponding E_g^{pure} values obtained with the WCGGA approximation and the mBJ method for the seven studied systems. These results demonstrate the general improvement in the prediction of the energy gaps with the mBJ method in comparison to WCGGA, as was shown in previous works for some pure alkali halides [22–24,30]. Therefore, the mBJ calculations, which are barely more expensive than those performed with the WCGGA approximation, are of relevant interest for our study of the defect levels induced by the anion vacancies in alkali halides.

3.2. The F-center

The *F*-center was produced by removing a halogen atom from a supercell of 2 × 2 × 2 times the primitive cell (vacancy atomic total dilution 1:64, see Fig. 3b). This neutral vacancy was treated using a sphere inside which the basis function is atom-like, as done for all the atoms in the structure (i.e., the vacancy is considered as a "ghost atom", without nucleus or electrons). In order to test the chosen APW + lo basis, additional calculations without the atomic sphere at the vacancy site were performed (i.e., treating the vacancy as part of the interstitial region). We found that both methods gave essentially the same results, but the use of the "ghost atom" located at the vacancy site allows the decomposition of the charge density at this site according to the different atomic-like orbitals of the basis. This helps to better understand the role of the vacancy by, for example, performing projections of the DOS at the vacancy site, as already presented in Fig. 4b–c and e–f for the atomic (cation and anion) sites in the perfect crystal.

For all the studied systems, the relaxation process was done using the WCGGA approximation, maintaining the symmetry of the vacancy site (O_h). Since WCGGA leads to reduced energy band-gaps with respect to the experimental values, the position of the defect electronic states introduced by the presence of the impurity is questionable. For this purpose, we used the mBJ

Table 1
Interionic distances d (in Å), experimental band-gap energy E_g, and absorption energy E_a for the studied systems. Predictions by WCGGA and mBJ for the energy gap for the pure crystal (E_g^{pure}) and the F-center system (E_g^{vac}), and the s-p transition energy (E_{sp}) are also listed. Energy values are expressed in eV.

System	d [25]	Experiment		WCGGA			mBJ		
		E_g^{exp} [26]	E_a	E_g^{pure}	E_g^{vac}	E_{sp}	E_g^{pure}	E_g^{vac}	E_{sp}
KI	3.53	6.0(1)	1.81(2)	4.0	4.3	1.5	6.0	6.1	1.9
KBr	3.30	7.4(2)	1.99(2)	4.4	4.7	1.6	7.3	7.3	2.3
KCl	3.15	8.4(2)	2.26(2)	5.1	5.4	1.8	8.6	8.8	3.0
NaCl	2.81	8.5(2)	2.66(2)	5.3	5.3	2.3	8.4	8.5	3.2
LiCl	2.56	9.4(1)	3.2 [2]	6.1	6.3	2.7	8.7	8.8	3.4
NaF	2.31	11.6(1)	3.61(2)	6.6	6.9	2.9	11.8	12.5	6.0
LiF	2.00	13.6(1)	4.94(2)	9.3	9.4	3.7	13.3	13.7	6.7

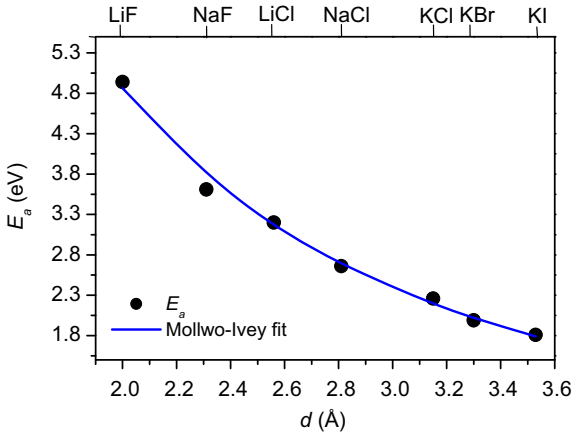

Fig. 2. Experimental absorption energy E_a as a function of the interionic distance d (the respective system names are indicated on the top). The blue solid line stands for best least-squares fit of the Mollwo-Ivey relation. (For interpretation of the references to colour in this figure legend, the reader is referred to the web version of this article.)

method, considering the positions of the atoms obtained after the full relaxation process with the WCGGA approximation. As our study is based in ground state calculations, there is no theoretical reason to expect that predictions for the energy transitions between vacancy levels agree exactly with the experimental absorption energies E_a. In this respect, many *ab initio* investigations were performed in order to deal with this issue [4,5,8,31,32] and, recently, different more sophisticated approaches for the treatment of the F-center absorption spectra than WCGGA and even mBJ have been proposed and compared in the LiF system [10]. In this work we focus only on the ground-state electronic structure modifications introduced by the anion vacancy over all the proposed alkali halide series.

The removal of the halogen atom in each case leads to structural distortions in the vicinity of the vacancy. According to the WCGGA calculations, the absence of an anion produces a displacement of the six nearest-neighbor cations outward the vacancy of about 1% of the lattice parameter, while the second neighbors (anions) slightly displace inwards the vacancy (changing its positions less than 0.5% of the lattice parameter). This behaviour can be understood in a simple Coulomb interaction scenario if the bound electron generates a weaker attractive force towards the NN cations than that performed by the removed halogen atom. It is worth to notice that, also in related fluoride materials, e.g. CaF_2, BaF_2, and SrF_2, relaxation of the first and second nearest neighbor atoms surrounding the F-center are smaller than 1% of the lattice constant parameter [11–13].

Fig. 5a shows the DOS for the NaCl supercell with a chlorine vacancy, obtained with the WCGGA approximation after the relaxation process. We found that this DOS is almost identical to that of the pure crystal (Fig. 4a). Therefore, the structural distortions induced by the vacancy do not produce significant changes in the DOS. For the system with vacancies, the valence band, dominated by the Cl-3p states, is separated of the conduction band by an energy gap E_g^{vac} of the same magnitude as that predicted for the pure system (5.3 eV, see Table 1). Fig. 5b and c shows the atom-projected partial DOS for Na and Cl, respectively. In these cases we selected the most distant atoms to the vacancy site (both at about 5 Å from the vacancy and with the major pure crystal-like contributions to the DOS). The vacancy induces the appearance of a partially occupied s-type donor level at about 1 eV below the conduction band minimum (see Fig. 5d). In addition, unoccupied

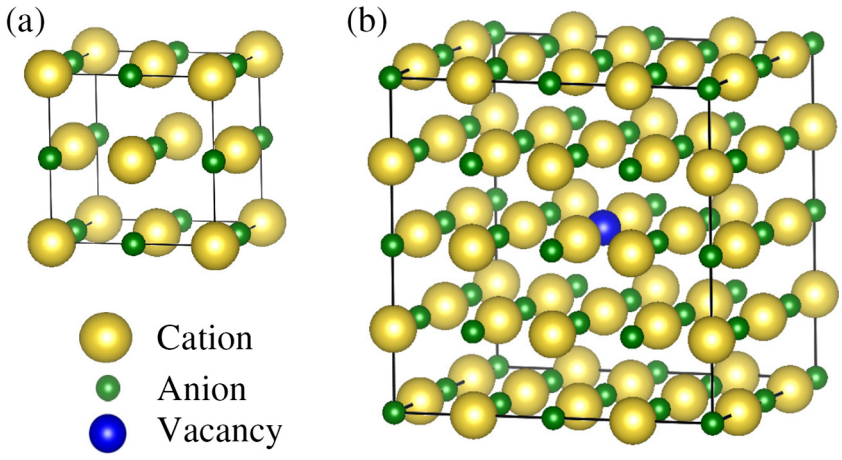

Fig. 3. Cubic NaCl unit cell (a) and 2 × 2 × 2 supercell with an anion vacancy (b).

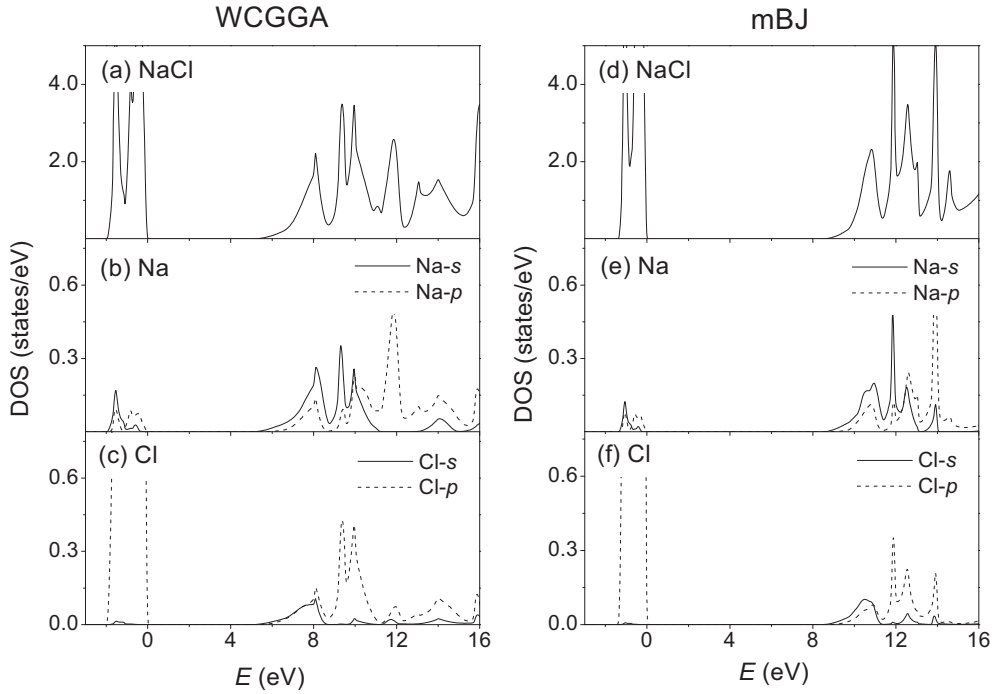

Fig. 4. Calculated total and atom-projected DOSs for pure NaCl predicted by the WCGGA approximation (a–c) and the mBJ method (d–f). For Na and Cl atoms the *s*-(*p*-) type contributions are presented with solid (dashed) lines. Different scales were used on the *y* axes to optimize visibility in all graphs. Energies refer to the highest occupied state.

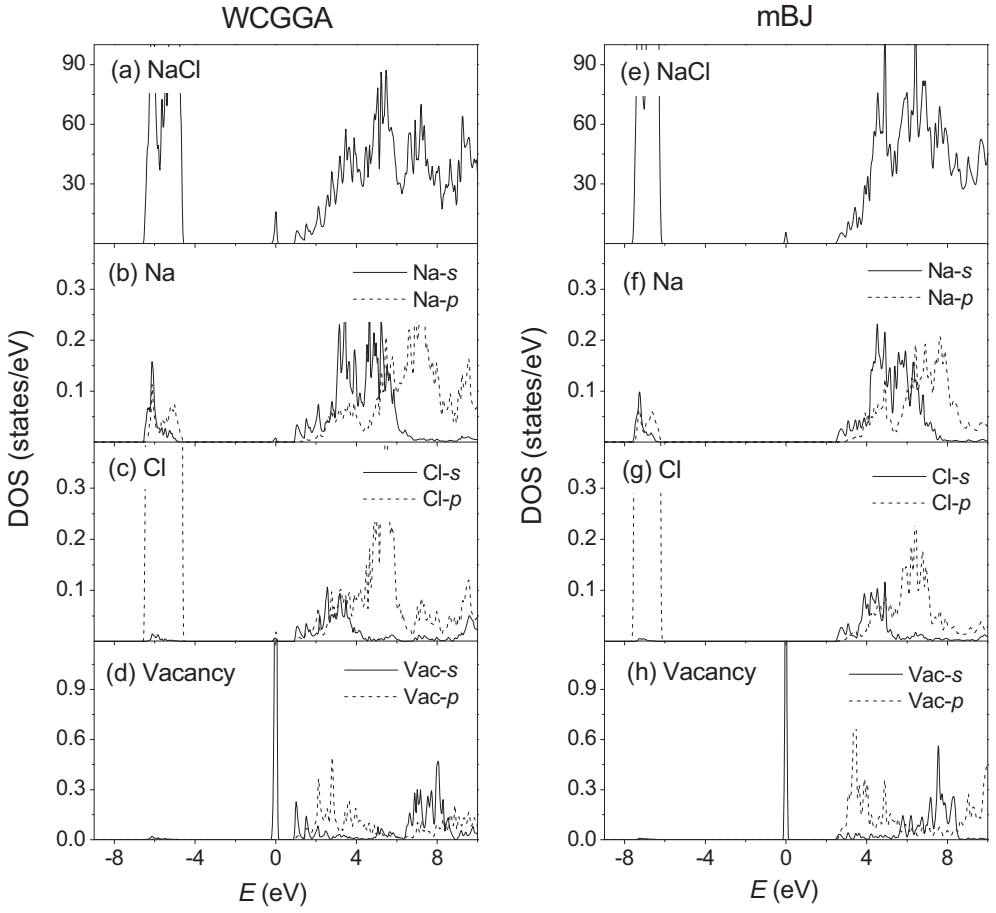

Fig. 5. Calculated total, atom-projected, and vacancy-projected DOSs for the NaCl supercell with an anion vacancy, predicted by the WCGGA approximation (a–d) and the mBJ method (e–h). For Na and Cl atoms, and for the vacancy sphere, the *s*-(*p*-) type contributions are presented with solid (dashed) lines. Different scales were used on the *y*-axes to optimize visibility in all graphs. Energies refer to the highest occupied state.

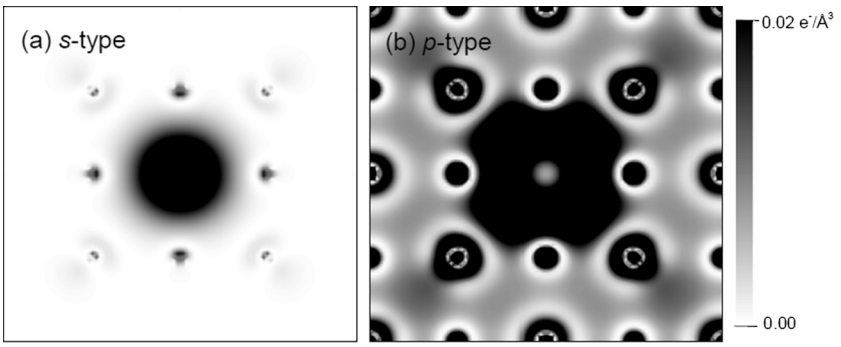

Fig. 6. Electron density projections for the vacancy electronic states in NaCl in the plane [1 0 0] and for states with energies in the range of the (filled) *s*-type state (a) and the (empty) *p*-type state (b) (see text). The vacancy site is at the center of each picture.

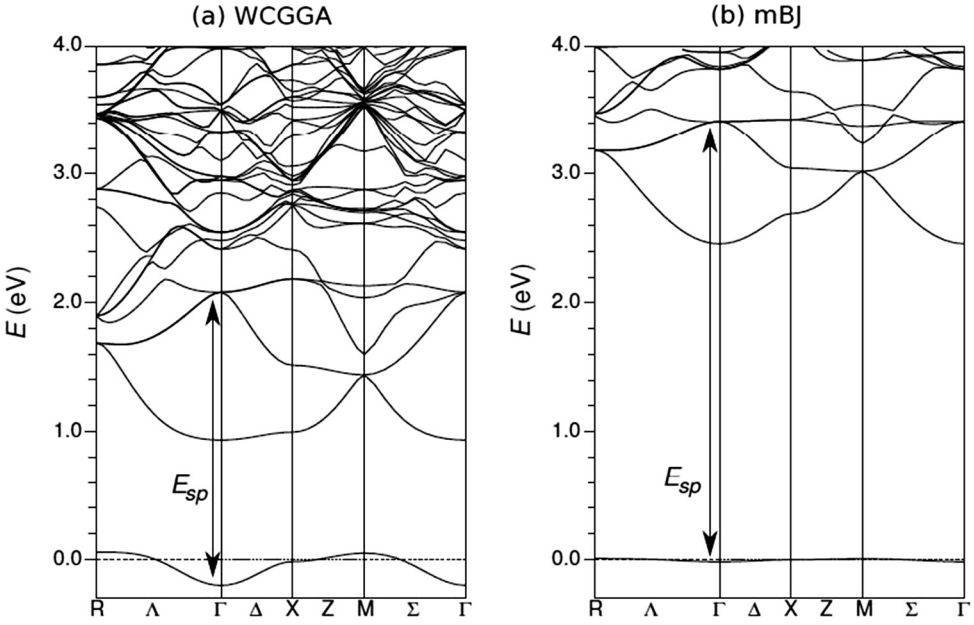

Fig. 7. Electronic band structure near the conduction band bottom for the NaCl supercell with an anion vacancy, calculated with the WCGGA approximation (a) and the mBJ method (b). The E_{sp} transition is at Γ point. Energies refer to the highest occupied state.

p-type vacancy states in the conduction band are found. The DOS obtained with the mBJ method for this system with vacancy presents the same features than those sketched in Fig. 5a-d, with differences arising from the prediction of a larger E_g value (E_g^{vac}=8.5 eV). It can be seen that this method increases the distance of the *s*-type vacancy state to the conduction band. Also, it is observed that the *p*-type vacancy states tend to localize on the conduction band bottom (Fig. 5h).

The spatial electron density projections corresponding to the states with energies in the range of the (filled) *s*-type and (empty) *p*-type vacancy levels are plotted in Fig. 6. At the center of each of these pictures is the vacancy site. The four nearest-neighbors are Na atoms (at ±*d* along the vertical and horizontal direction), and the next neighbors are Cl atoms (at $\sqrt{2}d$ from the vacancy site, along the diagonal). In Fig. 6a there are projected the 0.40 electrons that occupy the *s*-type donor level. This plot shows that the donor level found in the DOS (Fig. 5d) has a correspondence with a highly localized electron density distribution inside the vacancy site (i.e. a bounded electron) for the ground state. This good description to within two lattice parameter demonstrates that the proposed supercell approach is good enough to treat the *F*-center. In the same way, the first 0.4 electrons that occupy the energy range of the *p*-type states in the conduction band bottom are projected in Fig. 6b. In this case, it can be seen that those electrons are more delocalized.

The *s*-*p* energy difference (E_{sp}, for which we consider the first *p*-type peak inside the conduction band, see Fig. 5d and h) is 2.3 eV with the WCGGA approximation, and 3.2 eV with the mBJ method. In Fig. 7 we present the corresponding electronic band structures for NaCl, in an energy region that includes the vacancy donor level and the first states in the conduction band bottom. The E_{sp} energy corresponds to the $a_{1g} \rightarrow t_{1u}$ direct transition at the Γ point, and passes over the conduction band minimum, which does not have *p*-character (as shown in Fig. 5d and h). The calculated values of E_{sp} are in good agreement with the experimental absorption energy E_a (2.66(2) eV, see Table 1).

At this point it is important to mention that if we consider an indirect transition such as Γ → X or Γ → M, for which the final states have a weak *p*-type vacancy character, the corresponding transition energies are lower than E_{sp} (see Fig. 7). If we consider the WCGGA approximation, the mentioned indirect transitions start at 1.6 eV. Otherwise, if we consider the mBJ calculations, for the Γ → X transition we obtain 2.7 eV, which is 0.5 eV lower than the E_{sp} value. Because the E_{sp} prediction with the mBJ method over-

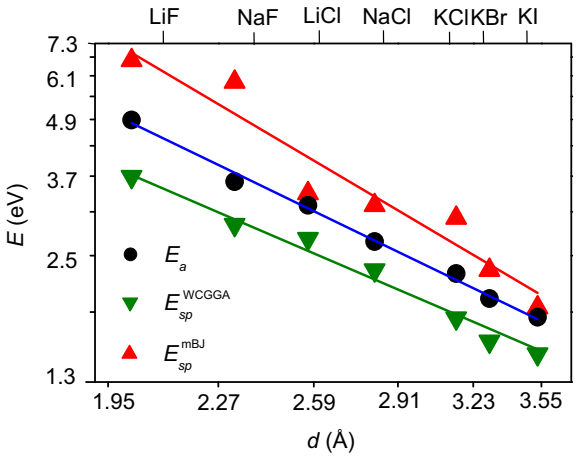

Fig. 8. Experimental absorption energy E_a and calculated E_{sp} energies as a function of the interionic distance d (the respective system names are indicated on the top). Solid lines are best least-squares fits of the Mollwo-Ivey relation for each data set (see text).

estimates E_a, by considering the indirect transitions predicted by this potential we found a better agreement with the measurements. This fact shows, as mentioned above, that the band gap problem strongly affects the correct description of the defect levels (as shown in Fig. 5). In this respect, other authors obtained similar predictions when used DFT methods that subestimate E_g [4,7]. Therefore, the use of a semilocal exchange and correlation potential as implemented in the mBJ method emerges as a more suitable procedure than the WCGGA for the description of these systems with vacancies. In this work we demonstrated that the mBJ method gives an accurate prediction of the E_g value, and simultaneously rearranges the relative position of the *s*- and *p*-type vacancy states, giving E_{sp} values in a better agreement with the experimental energy E_a than those calculated with WCGGA.

In Table 1 we list the E_g^{vac} and E_{sp} energies for all the studied systems with an anion vacancy, obtained by WCGGA and mBJ. Both energies increase with decreasing the interionic distance d. As can be seen in Table 1, in general, the energy gaps of the system with vacancy (E_g^{vac}) are slightly larger than those of the pure compound (E_g^{pure}), being the differences between them below 8%. Concerning E_{sp}, for KI the difference between the predictions obtained by both methods is minimum (0.4 eV), and for NaF and LiF (which have the minimum distances d among the studied alkali halides) this difference reaches its maximum (3.1 and 3.0 eV, respectively). Depending on the studied compound and the method of calculation, the predicted E_{sp} energy represents 30–50% of E_g^{vac}, and by mBJ the E_{sp}/E_g^{vac} ratio decreases monotonously with d. Additionally, it can be noted that the distance from the a_{1g} level to the conduction band minimum (at Γ point, see Fig. 7) also decreases monotonously with d. If we compare our theoretical predictions with the experimental measurements, the E_{sp} energies obtained by WCGGA subestimate the absorption energy E_a (E_{sp} values are 15–25% lower than E_a), while by mBJ the E_{sp} energies overestimates E_a (E_{sp} values are 5–66% higher than E_a). However, as we concluded for NaCl, considering the possible indirect transitions, the latter method is more suitable for the comparison with experimental results. Fig. 8 shows the results for the experimental E_a and the theoretical E_{sp} energies as a function of d, and the corresponding power-law relation fits. We obtain for the WCGGA calculations $E_{sp}^{WCGGA}(d) = 12(1)\ d^{-1.6(1)}$, and for the mBJ method $E_{sp}^{mBJ}(d) = 31(8)\ d^{-2.2(3)}$, where d is expressed in Å and E_{sp} in eV. These relations agree with the experimental trend obtained for $E_a(d)$ and delimit the Mollwo-Ivey relation of Eq. (1). For the mBJ method, the predicted $E_{sp}^{mBJ}(d)$ power-law relation is in perfect agreement with the simpler models based in a Schrödinger-like problem of an electron trapped in a potential well (according to this treatment E_a has d^{-2} dependence), which were often proposed in the very beginning of the study of these systems [2,33]. However, the success of this non-*ab initio* models depends on arbitrary values for the potential width and depth.

4. Summary and conclusions

We revisited experimentally the characterization of the absorption energies E_a in *F*-centers in alkali halides, and we analysed by first-principles the structural and electronic properties of the anion vacancy. Using the proposed supercell approach with an atomic sphere description of the vacancy site ("ghost atom" approach), we demonstrated that the bounded electron is localized to within two lattice parameter. We observed that the structural distortions induced by the vacancy do not affect significantly the DOS of the studied compounds, except for the introduction of the donor vacancy states. For all the studied systems with vacancies, an *s*-type defect level is found isolated, near the conduction band minimum, together with the *p*-type states localized at the bottom of the conduction band. We showed that the mBJ method performs accurate predictions for the energy band gap E_g and gives values for the *s*-*p* transition energies in better agreement with the experimental E_a than those obtained with WCGGA.

Acknowledgements

This work was partially supported by Consejo Nacional de Investigaciones Científicas y Técnicas (CONICET) under Grant No. PIP0803, Argentina. This research made use of the computational facilities of the Physics of Impurities in Condensed Matter (PhI) group and the HPPC BOSE Cluster at IFLP and Departamento de Física (UNLP). The Chemistry Department (Facultad de Ciencias Exactas, UNLP) is kindly acknowledged for facilitating the UV/VIS experimental facilities. DR and MR (JH) are (is) members (fellow) of CONICET, Argentina.

References

[1] C. Kittel, Introduction to Solid State Physics, fifth ed., Wiley, 1976.
[2] J.J. Markham, in: F. Seitz, D. Turnbull (Eds.), F-centers in alkali halides, Academic Press, 1966.
[3] M.S. Malghani, D.Y. Smith, Phys. Rev. Lett. 69 (1992) 184–187.
[4] M.R. Pederson, B.M. Klein, Phys. Rev. B 37 (1988) 10319–10331.
[5] M.P. Surh, H. Chacham, S.G. Louie, Phys. Rev. B 51 (1995) 7440–7464.
[6] R.F.W. Bader, J.A. Platts, J. Chem. Phys. 107 (1997) 8545–8553.
[7] C.M. Fang, R.A. De Groot, J. Phys.: Condens. Matter 20 (2008) 075219.
[8] W. Chen, C. Tegenkamp, H. Pfnür, T. Bredow, Phys. Rev. B 82 (2010) 104106.
[9] C. Ma, T. Liu, Q. Chang, Comp. Theor. Chem. 1080 (2016) 79–83.
[10] F. Karsai, P. Tiwald, R. Laskowski, F. Tran, D. Koller, S. Gräfe, J. Burgdöfer, L. Wirtz, P. Blaha, Phys. Rev. B 89 (2014) 125429.
[11] H. Shi, L. Chang, R. Jia, R.I. Eglitis, J. Phys. Chem. C 116 (2012) 4832–4839.
[12] H. Shi, R. Jia, R.I. Eglitis, Solid State Ion. 187 (2011) 1–7.
[13] H. Shi, L. Chang, R. Jia, R.I. Eglitis, Comput. Mater. Sci. 79 (2013) 527–533.
[14] R.I. Eglitis, N.E. Christensen, E.A. Kotomin, A.V. Postnikov, G. Borstel, Phys. Rev. B 56 (1997) 8599.
[15] D. Ricci, G. Bano, G. Pacchioni, F. Illas, Phys. Rev. B 68 (2003) 224105.
[16] E. Cho, S. Han, H. Ahn, K. Lee, S.Keun Kim, C.Seong Hwang, Phys. Rev. B 73 (2006) 193202.
[17] A.F. Fix, F.U. Abuova, R.I. Eglitis, E.A. Kotomin, A.T. Akilbekov, Phys. Scr. 86 (2012) 035304.
[18] M. Gerosa, C.E. Bottani, L. Caramella, G. Onida, C. Di Valentin, G. Pacchioni, J. Chem. Phys. 143 (2015) 134702.
[19] P. Blaha, K. Schwarz, G.K.H. Madsen, D. Kvasnicka, J. Luitz, WIEN2k, An Augmented Plane Wave + Local Orbitals Program for Calculating Crystal Properties, Karlheinz Schwarz, Techn. Universität Wien, Austria, 2001.
[20] Z. Wu, R.E. Cohen, Phys. Rev. B 73 (2006) 235116.
[21] I.N. Yakovkin, P.A. Dowben, Surf. Rev. Lett. 14 (2007) 481–487.
[22] F. Tran, P. Blaha, Phys. Rev. Lett. 102 (2009) 226401.
[23] D. Koller, F. Tran, P. Blaha, Phys. Rev. B 85 (2012) 155109.
[24] J.A. Camargo-Martínez, R. Baquero, Phys. Rev. B 86 (2012) 195106.

[25] R.W.G. Wyckoff, Crystal Structures, vol. 1, 2nd ed., Wiley, 1965.
[26] R.T. Poole, J.G. Jenkin, J. Liesegang, R.C.G. Leckey, Phys. Rev. B 11 (1975) 5179–5189.
[27] W.Y. Ching, F. Gan, M.Z. Huang, Phys. Rev. B 52 (1995) 1596–1611.
[28] P.K. de Boer, R.A. de Groot, Am. J. Phys. 67 (1999) 443–445.
[29] P.K. de Boer, R.A. de Groot, Phys. Lett. A 256 (1999) 227–229.
[30] H. Jiang, J. Chem. Phys. 138 (2013) 134115.
[31] J. Carrasco, C. Sousa, F. Illas, P.V. Sushko, A.L. Shluger, J. Chem. Phys. 125 (2006) 074710.
[32] P. Rinke, A. Schleife, E. Kioupakis, A. Janotti, C. Rödl, F. Bechstedt, M. Scheffler, C.G. Van de Walle, Phys. Rev. Lett. 108 (2012) 126404.
[33] J.F. Reichert, Am. J. Phys. 51 (1983) 431–433.